Caisson Foundation Response During Liquefaction Induced Lateral Spreading

Shibayan Biswas and Deepankar Choudhury

Abstract Caisson foundations are widely used as the foundation system of bridges, transmission towers, and scour vulnerable structures for transmitting high structural load to the soil beneath. In seismically active regions having potentially liquefiable soils, one important consideration is the effect of liquefaction induced lateral spreading on deep foundations. During this phenomenon, caissons are subjected to seismic forces and simultaneously it loses the lateral support of surrounding soil due to liquefaction and an extra kinematic loading acts because of the flow of the liquefied soil. In this present study, a caisson embedded in liquefiable soil in gentle sloppy ground has been modeled in finite element-based software package PLAXIS 3D for capturing the response of the caisson in laterally spreading ground. The proposed numerical model has been found to compare well with the available centrifuge test results. Further parametric study has also been performed for lateral response of the caissons in liquefying soil for different ground slopes, embedment depth to caisson width ratio, frequency and amplitude of the dynamic motion. Behavior of the rigid caisson foundations subjected to liquefaction induced kinematic loading have been thoroughly discussed in the present study to assist the seismic design of caissons embedded in potentially liquefiable soil.

Keywords Caisson · Liquefaction · Lateral spreading · Kinematic

1 Introduction

Liquefaction-related phenomenon is associated with rapid loss of strength and stiffness of soil due to application dynamic loading. The excess pore pressure generated due to vibrations compensates the total stress in soil and the soil starts flowing like a viscous fluid. Whether the soil has been fully liquefied or not that can be estimated from the value of excess pore pressure ratio (r_u) of soil which is defined as

S. Biswas (✉) · D. Choudhury
Department of Civil Engineering, IIT Bombay, Powai, Mumbai 400076, India

D. Choudhury
e-mail: dchoudhury@iitb.ac.in

the ratio of excess pore pressure to in-situ vertical effective stress. A r_u value of 1.0 (practically r_u value above 0.9–0.95) suggests full liquefaction. Liquefaction induced lateral spreading is mainly common in gentle sloping grounds and can be significant for partially liquefied soil also. When the reduced strength of slope soil falls below the static strength required to maintain the equilibrium in slopes, lateral spreading occurs. According to NCEER-92 workshop, lateral spreading generally occurs in 0.3–5% slopes [1], though, many researchers have suggested that it occurs in grounds having slope between 1° and 5°. Effect of kinematic loading on pile response due to lateral spreading has been investigated throughout the years using different methodologies such as force equilibrium method, p-y method, and finite element method. However, a very limited amount of work has been found on the lateral response of caisson foundation during lateral spreading condition. Due to the large cross-sectional area with high rigidity, caisson foundations were generally believed to have high capacity against the axial as well as the lateral loading and subsequently immune to seismic loading. However, this assumption was found to impart a fallacious hope only after several bridges founded on caisson foundations were reported to encounter damage in Kobe 1995 earthquake [2, 3]. Previous researchers [4, 5] have reported the girder failure of Nishinomiya-Ko Bridge and abutment failure of Kobe Bridge which occurred after Kobe 1995 earthquake. Although the caisson itself was found to be more or less unaffected, but bridge failure occurred due to displacement or rotation of caisson in the direction of laterally spreading soil. Therefore, the necessity for providing a systematic design guideline for caisson foundation design is instituted specifically for estimating the pressure coming from the flowing soil in lateral spreading phenomenon.

In the present study, numerical analysis using PLAXIS 3D [6] has been performed to investigate the different aspects of caisson-soil interaction under the liquefaction induced lateral spreading condition. The suitable constitutive model which can capture the liquefaction phenomenon as well as post liquefaction scenario has been discussed. The proposed model has been validated with the centrifuge test results and the results simulated by the proposed model has been found to be in good agreement with the available experimental results. After validation of the numerical model, detailed parametric study has been performed to observe the response of caissons embedded in liquefying soil for different frequency, amplitude of input dynamic motions, different ground slopes, and various caisson depth to width ratio.

2 Numerical Approach

2.1 Details of Numerical Methodology

A numerical method using finite element-based software package PLAXIS 3D [v.2018.01 (PLAXIS3D, 2018)] [6] has been adopted in this present study for simulating the effect of lateral spreading on a rigid caisson embedded in liquefying soil. A

3D model has been formed to capture the complete soil-structure interaction around the caisson. The optimized model dimensions were used for this analysis to ensure the non-significant effect of wave reflections. Free-field boundary condition has been used at the vertical sides of the boundary by employing free-field elements. Using this boundary condition, the free-field motion is transformed to the main domain by applying equivalent forces at the boundary. At the bottom of the 3D model, compliant base boundary condition has been employed to account for both absorption and application of dynamic input. The 3D soil and caisson elements have been modeled as 10-noded tetrahedral elements and the interface elements are modeled as 12-noded elements. In this analysis, caisson foundations have been modeled as rigid body where the relative displacement and angle between two points remain same before and after application of loads. That means the caisson will undergo rotation and/or translation depending upon the type of loading, but will not bend with respect to its longitudinal axis. This replicates the massive and heavy caisson of large dimensions with high stiffness contrast between caisson and soil. Ground water table has been considered at surface parallel to inclined ground and no slip condition at interface has been considered. An undrained analysis has been performed for the liquefaction problem. To facilitate free flow of soil during lateral spreading, the top ground surface has been kept in inclination with a certain percent of slope with the horizontal line throughout the domain. Therefore, the height of the soil block at two opposite ends has been kept at different elevations with the direction of slope staying along the direction of input motion (see Fig. 1).

In this dynamic analysis, damping has been incorporated inside the soil model through frequency dependent Rayleigh damping formulation, which can be defined as

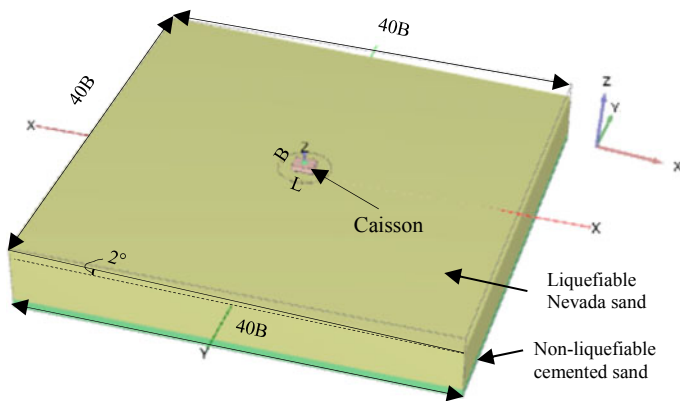$$2\omega\xi = \alpha + \beta\omega^2 \tag{1}$$

Fig. 1 3D model with slope used in the numerical analysis

$$\omega = 2\pi f \tag{2}$$

where ξ is the damping ratio, ω is the angular frequency and f is the frequency of input motion, α, β are Rayleigh damping coefficients. Two target frequencies (ω_1, ω_2) and their corresponding damping ratios (ξ_1, ξ_2) were set to compute the damping coefficients as below.

$$\alpha = 2\omega_1\omega_2 \frac{\omega_1\xi_2 - \omega_2\xi_1}{\omega_1^2 - \omega_2^2} \tag{3}$$

$$\beta = 2\frac{\omega_1\xi_1 - \omega_2\xi_2}{\omega_1^2 - \omega_2^2} \tag{4}$$

Generally, 1st and 2nd mode of natural frequencies are considered as the two target frequencies. In the analysis, 10% damping has been considered which is consistent with the practical range for soils. Sensitivity analyses of meshing have been performed to ensure optimized mesh density where both accuracy as well as numerical cost effectiveness were taken care off. The mesh size has been checked for the required element size from the time step calculation and seismic wave propagation criteria.

UBC3D PLM. To capture the rapid excess pore water pressure buildup and subsequent decrease in soil strength, a constitutive model named UBC3D-PLM has been used in this study. This model is generalized 3-D upgradation of UBCSAND model (University of British Columbia Sand) which was formulated by UBC researchers. Like UBCSAND, UBC3D-PLM is an effective-stress-based elasto-plastic model which follows the axioms of classical plasticity theory and consists of different rules for predicting soil behavior. A densification rule associated with secondary yield surface has been introduced in the UBC3D-PLM to simulate the generation of excess pore pressure with reasonable accuracy. To incorporate the degradation of stiffness after reaching liquefaction, i.e., post liquefaction phenomenon, a dilation factor has also been introduced in this model which can capture the gradual degradation of plastic shear modulus due to generation of plastic deviatoric strain at the time of dilation. Initially [7] performed several triaxial tests on soil response and proposed the equations for computation of parameters used for UBC3D-PLM. In their companion paper, [8] validated those expressions and proposed the modified expressions, mainly based on the in-situ corrected SPT value. In this present study, the constitutive model parameters are computed from the available relations provided by different researchers. Their proposed relations are based on the tests performed on the typical types of soils and for capturing a particular nature of soil. It is always advisable to perform tests for the model parameters evaluation for the response the researcher want to capture. In absence of test results, these relations can provide better estimate.

Fig. 2 Input motion used in
the centrifuge experimental
setup [9]
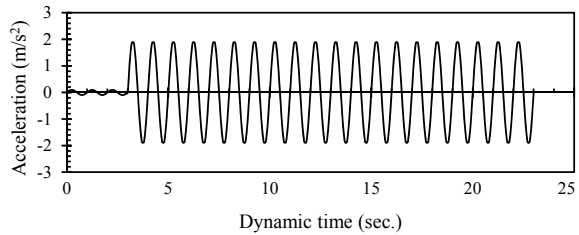
2.2   Validation of the Numerical Methodology

The proposed model is compared with the results found from the experiment
performed by [9] in centrifuge at 50-g condition as a part of a NEES study at RPI.
The stiff rigid caisson was made of aluminum which has external dimensions of 5 ×
3.65 × 15.2 m in prototype. The soil layer consists of 10 m of potentially liquefiable
Nevada sand with 2 m of bottom sand mixed with 5% Portland cement which provides
soil-soil interaction with liquefiable soil and dense kind of behavior of bottom sand.
The caisson was restrained at bottom to provide extra rotational stiffness. The whole
container was kept at 2° with horizontal to facilitate lateral spreading. The similar
condition has been replicated in PLAXIS 3D software. The depth of soil at one side
was 10 m where in another side, it was 15.23 m to maintain the 2° slope throughout
the soil domain (see Fig. 1). The input motion which was applied at bottom base
consists of 3 low amplitude cycles of ±0.01 g and followed by 20 high amplitude
cycles of ±0.2-g with a frequency of 1 Hz at prototype. Figure 2 shows the motion
which was applied in the direction of lateral displacement.

   The far-field displacement, excess pore water pressure variation, base acceleration
with dynamic time, upslope passive earth pressure distribution along caisson depth,
as shown in [9] and in their companion paper [10], have been generated in the
numerical analysis and compared thoroughly. From Fig. 2, it can be seen that far-field
displacement, excess pore pressure at different depths, and base acceleration at far-
field location are in good agreement with the results obtained from [10]. Further, the
variation of upslope passive pressure along the depth of caisson has been compared
well with [9] result. Therefore, the suitable selection of UBC3D-PLM model in this
numerical analysis to capture the liquefaction and post-liquefaction phenomenon has
been found to work well (Figs. 3 and 4).

3   Parametric Study

After validation of the proposed model, a detailed parametric study has been
performed. Various parameters such as depth of liquefiable soil, caisson height to
width ratio, slope of ground to initiate lateral spreading post-liquefaction have been
varied. In this study, four different types of sinusoidal motion covering the probable
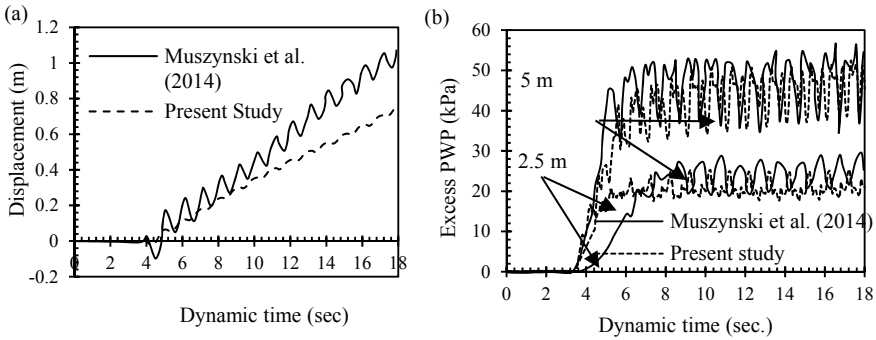
Fig. 3 Comparison of the numerical analysis results with the available centrifuge test results: **a** surface displacement at far-field location, **b** excess pore pressure at far-field location for 2.5 and 5 m depth from the ground surface

Fig. 4 Comparison of upslope passive pressure distribution obtained from the numerical analysis with the centrifuge test results
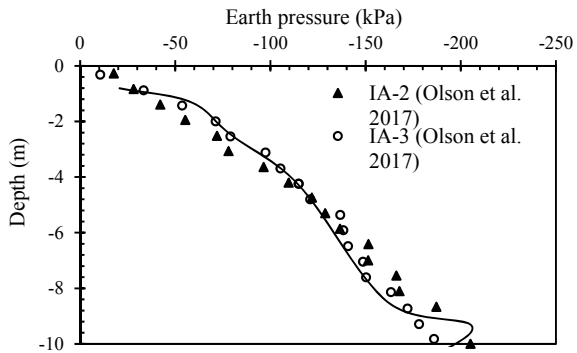

range of frequencies and amplitudes were used to observe the response of the caissons for different scenarios. Table 1 shows the details of the motions used in this analysis. Two different ground slope, i.e., 1% and 4% have been used in the present study and have been denoted as S1 and S4, respectively, for the rest of the paper. Soil properties have been kept same as used in the numerical analysis performed for validation.

Figure 5 shows that liquefaction has occurred for all the loading conditions. It

Table 1 Different types of input motion used in the parametric study

No	Frequency (Hz)	Amplitude (g)	Notation
1	2	0.4	M1
2	2	0.1	M2
3	1	0.4	M3
4	1	0.1	M4

(a)

(b)

(c)

(d)
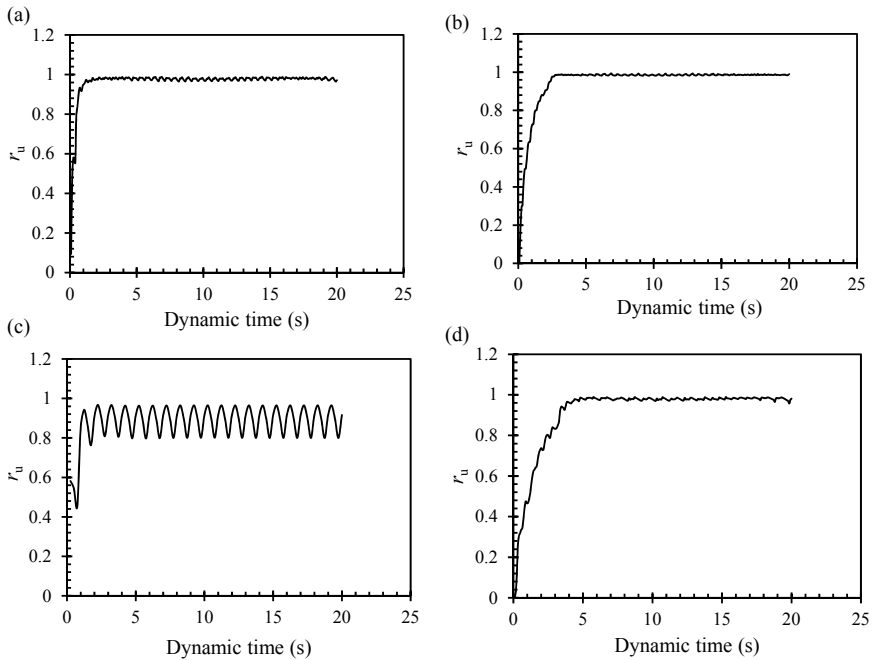
Fig. 5 Typical r_u versus dynamic time plot for **a** M1, **b** M2, **c** M3, **d** M4 motions for S1 ground slope inclination

also has been observed that for same motion frequency, if amplitude increases lique-faction occurs earlier as the cyclic shear stress applied is higher for higher amplitude motion. Also, liquefaction triggering depends on no. of stress reversals. Henceforth for same amplitude, no. of stress reversals increases with increment of frequency and subsequently liquefaction triggers earlier (see Fig. 5c, d).

Free-Field Displacement. Previous studies recommended that the response of deep foundations subjected to kinematic loading can be defined more profoundly by calculating the transfer function which is a ratio of the free-field ground displace-ment and foundation displacement. Present study indicated an increment in free-field displacement as the slope inclination increases. It can be due to the fact that with greater slope inclination, the driving stress for the flow of the soil increases which results in more displacement. Similar phenomenon can be observed for an increment of motion amplitude. However, the free-field displacement can be seen to decrease as the frequency of the input motion increases.
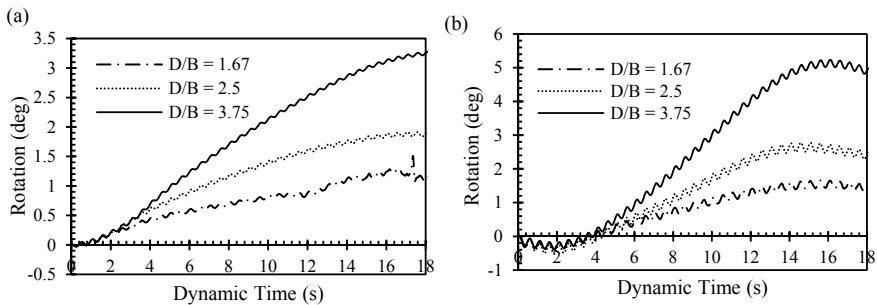
Caisson Response—Displacement and Rotation. Top head displacement and rotation of caisson are two major factors for the stability of caisson foundations subjected to lateral loading and have been investigated in the present study. Slender foundations like pile could follow more or less the wavy motion of the ground caused by the seismic waves. However, rigid foundations with high stiffness contrast compared to the surrounding soil generally don't follow free-field movement and

tend to modify the soil deformation. Henceforth the displacement of the caisson can be seen to be much different from the free-field ground motion. This phenomenon is known as the kinematic filtering effect of rigid foundations such as caissons. This filtering effect becomes more prominent for the foundations having high bending rigidity and low value of slenderness ratio. This can be compared in terms of wavelength of seismic shear waves in the soil and dimensions of a caisson, i.e., from the λ_{ff}/L value. Where λ_{ff} is the wavelength of the seismic wave which can be defined as V_s/f and L is caisson length. V_s is the shear wave velocity of the soil and f is the frequency of the input motion.

From Fig. 6, it can be observed that the caisson head displacement increases for increasing D/B ratio for S1 ground slope. Similar pattern has been found for the caisson embedded in S4 ground slope (see Fig. 7). According to the available literature, if λ_{ff}/L value decreases, the filtering effect of the caisson increases and the displacement of caisson decreases. For the same reason the rotation of the caisson reduces. That is why for D/B ratio of 3.75, the displacement and rotation is more. Though for D/B ratio of 2.5 and 1.67, the caisson height is same, but for D/B ratio
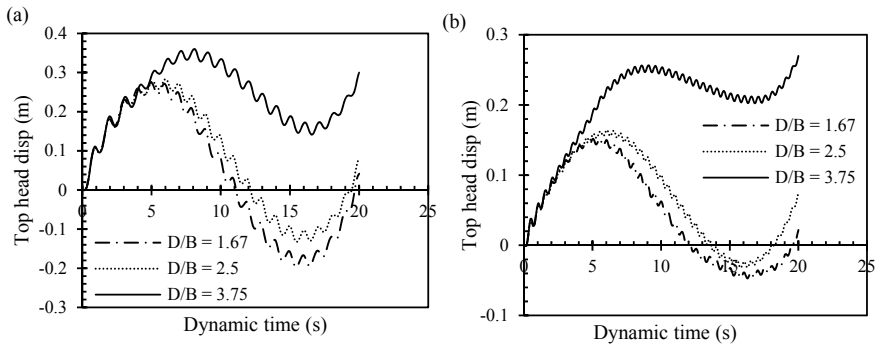

Fig. 6 Typical variation of top head displacement of caisson for 1% slope inclination (S1) for **a** M4 motion, **b** M2 motion


Fig. 7 Typical variation of caisson rotation for 4% slope inclination (S4) for **a** M2 motion, **b** M1 motion

of 1.67, the caisson width is more. This may be affecting the response and predicts less displacement and rotation for D/B ratio of 1.67. Figure 8 shows that the top head displacement and rotation of caisson increase as the slope inclination increases. This is due to the higher driving stress for the flow of the soil as discussed earlier. The effect of amplitude of input motion on caisson head displacement and rotation of caisson have been presented in Fig. 9. The top head displacement and rotation of the caisson increases with the increase in amplitude of the input motion. As the amplitude of the motion increases, the force imposed on the caisson increases which results in more displacement and rotation.
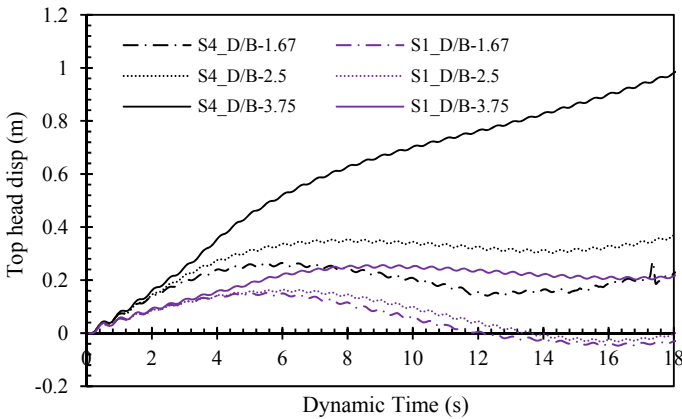
Fig. 8 Effect of ground slope inclination on top head displacement of caisson for M2 motion
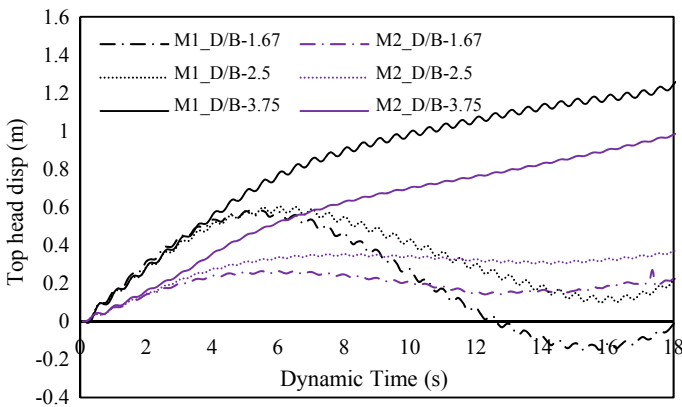
Fig. 9 Effect of amplitude of input motion on top head displacement of caisson for 4% ground slope inclination (S4)

4 Conclusions

This study presents the response of caisson foundations in liquefaction induced lateral spreading phenomenon in a qualitative way. Rigid foundations with high stiffness contrast compared to the surrounding soil generally don't follow free-field movement and tend to filter the soil deformation. Therefore, the caisson itself may be more or less unaffected due to the impact of lateral loading unlike piles but the slight movement and/or rotation of caisson due to the lateral flow pressure coming from the sub-soil ground movement initiates the failure of super-structures and subsequent damages. User defined PLAXIS 3D model UBC3D-PLM which can successfully capture the liquefaction phenomenon and flow of soil due to lateral spreading phenomenon has been used in the numerical analysis. This constitutive model is popular for its simplicity as well as for its effectiveness for successful prediction of soil behavior like triggering of liquefaction, post-liquefaction behavior, cyclic mobility, etc., using numerical and finite element formulation. The loss in capacity of surrounding soil due to seismically induced liquefaction when the caisson is has been found to affect the lateral stability of caissons embedded in potentially liquefiable soil through increase in top head displacement and rotation. The effect of different parameters on the extent of lateral spreading phenomenon which in turn affects the response of caisson has been observed through far-field ground displacement. The free-field displacement increases with slope, amplitude, and frequency of the input dynamic motion. It has also been observed that both the caisson head displacement and rotation increase for increase in amplitude of input motion, ground slope, caisson embedment to width ratio and decreases with the frequency of the input motion. The discussion on the behavior of the rigid caisson foundations subjected to liquefaction induced kinematic loading can be considered to provide the initial steps for the seismic design of caissons embedded in potentially liquefiable soil.

References

1. Youd TL (1978) Major cause of an earthquake damage is ground failure. Civil Eng ASCE 47–51
2. Biswas S, Choudhury D (2019) Seismic soil resistance for caisson design in sand. Proc Inst Civ Eng Geotech Eng 172(1):67–75
3. Biswas S, Choudhury D (2020) Caissons in cohesionless soils considering 3D wedge under earthquake loading. Int J Geomech 20(12):04020221
4. Finn WD, Thavaraj T (2001) Deep foundations in liquefiable soils: case histories, centrifuge tests and methods of analysis. In: Proceedings of international conferences on recent advances in geotechnical earthquake engineering and soil dynamics, USA
5. Matsui T, Oda K (1996) Foundation damage of structures. Soils Found 36(Special):189–200
6. Plaxis BV (2018) Netherlands user manuals. Plaxis 3D
7. Makra A (2013) Evaluation of the UBC3D-PLM constitutive model for prediction of earthquake induced liquefaction on embankment dams. MSc thesis, TU Delft
8. Petalas A, Galavi V (2013) Plaxis liquefaction model UBC3DPLM. Plaxis Rep

9. Olson SM, Hashash YM, Muszynski MR, Phillips C (2017) Passive wedge formation and limiting lateral pressures on large foundations during lateral spreading. J Geotech Geoenvironmental Eng 143(7):04017027
10. Muszynski MR, Olson SM, Hashash YM, Phillips C (2014) Repeatability of centrifuge tests containing a large, rigid foundation subjected to lateral spreading. Geotech Test J 37(6):1002–1015